J Mater Sci (2010) 45:3874–3881
DOI 10.1007/s10853-010-4445-0

Microplasticity phenomena in thermomechanically strained nickel thin films

A. A. Taylor · S. H. Oh · G. Dehm

Received: 22 October 2009 / Accepted: 26 March 2010 / Published online: 6 April 2010

Abstract Magnetron sputtered Ni thin films on both oxidised Si (100) and α-Al_2O_3 (0001) substrates of thickness 150–1000 nm were tested thermomechanically with a wafer curvature system, as well as in situ in a transmission electron microscope. The films on oxidised Si have a {111}-textured columnar microstructure with a mean grain size similar to the film thickness. On (0001) α-Al_2O_3 a near single crystal epitaxy with two growth variants is achieved leading to a significantly larger grain size. The thermomechanical testing was analysed in terms of the room temperature/high temperature flow stresses in the films and the observed thermoelastic slopes. It was found that the room temperature flow stresses increased with decreasing film thickness until a plateau of $\sim$1100 MPa was reached for films thinner than 400 nm. This plateau is attributed to the present experiments exerting insufficient thermal strain to induce yielding in these thinner films. At 500 °C the compressive flow stresses of the films show a competition between dislocation and diffusion mediated plasticity. A size effect is also observed in the thermoelastic slopes of the films, with thinner films coming closer to the slope predicted by mismatch in thermal expansion coefficients. It is put forward here that this is due to a highly inhomogeneous stress distribution in the films arising from the grain size distribution.

A. A. Taylor (✉) · G. Dehm
Erich Schmid Institute of Materials Science, Austrian Academy of Sciences, Jahnstraße 12, 8700 Leoben, Austria
e-mail: aidan.a.taylor@gmail.com

S. H. Oh
Department of Materials Science and Engineering, Pohang University of Science and Technology, Pohang 790-784, Korea

G. Dehm
Department Materials Physics, Montanuniversität Leoben, Jahnstraße 12, 8700 Leoben, Austria

Introduction

As devices such as microprocessors and their associated electronics, as well as microelectromechanical systems reduce in size and become more complex the individual features in their construction enter the micro- and nanometer scale. Microprocessors now contain features less than 50 nm in size. It is, however, known [1] that metals, such as those used in the metallisation lines of said devices, do not behave in the same way on this sub-micron size scale as a scaling-down of bulk mechanical properties would predict. In particular, metals regularly exhibit a higher yield stress when tested in very small dimensions, e.g. [2–5], significantly exceeding predictions by the Hall-Petch relation [6, 7].

Due to the mismatch in thermal expansivity between these metal thin films/structures and the substrates onto which they are deposited it is very common for large stresses to be present in the films. The high stresses in these films, combined with the modification in their mechanical properties compared to bulk materials, can lead to the unpredicted failure of these devices [8]. It is therefore important to understand the small-scale mechanical properties of metals in order to provide improved, less failure prone, device design.

There are, in fact, two components to an investigation of metallic structures on this length-scale; the microstructure and the thermomechanical properties. The microstructure of thin metallic films depends on several factors including deposition temperature, substrate material and film thickness [9–11]. It is therefore important to have a thorough

understanding of this prior to any investigation of the thermomechanical properties.

Theoretical models have been proposed to determine the physical processes taking place in the metal films during thermomechanical testing. By comparing the stress–temperature cycles produced by assuming various active physical processes with those cycles recorded experimentally an insight into the mechanisms at work in these films can be gained. In particular, the Nix–Freund model [1, 12] of dislocation glide on inclined planes, Gao's model [13, 14] of constrained diffusional creep and von Blanckenhagen's [15] model of source activation have shown considerable success at producing quantitative agreement between experiment and theory.

All these models aim to explain the global stress evolution in thin films by considering the effect of local events averaged out over the whole film. In doing so it is assumed that the microstructure can be approximated to a single crystal, in the case of the Nix–Freund model [1, 12], or a polycrystal of uniform grain size in the work of von Blanckenhagen [15] and Gao [13, 14]. The distribution of grain sizes present in thin films and conductor lines does, however, lead to some material effects that cannot be explained by these models as plastic deformation will tend to be localised in the more favourably sized and oriented grains.

The Ni films studied here have been characterised in a similar manner to previous work in the area but in addition a focus is placed on how small and large grains in the films affect the plastic properties and the thermoelastic slopes of the stress–strain curves. In situ transmission electron microscopy (TEM) was utilised to further investigate these local phenomena in the 200-nm-thick polycrystalline Ni film.

Experimental

Film deposition[1]

The films examined in this study were produced by magnetron sputtering onto (0001)-oriented α-Al_2O_3 (50 mm diameter, 330 μm thickness) in the case of the epitaxial films while the polycrystalline films were deposited onto (001)-oriented Si wafers (50 mm diameter, 280 μm thickness). The Si substrates were coated with a 100 nm amorphous SiN_x/amorphous SiO_x bilayer such that interdiffusion between metal and substrate is inhibited. The amorphous SiN_x/SiO_x bilayer prevents epitaxy between Ni and Si and leads to a polycrystalline microstructure. The substrates were mounted in an ultrahigh vacuum (UHV) deposition system where they were Ar^+ sputter-cleaned (10^{-2} Pa Argon pressure, 100–500 eV kinetic energy) to remove surface contaminants. Film deposition was achieved using a magnetron sputtering system (DCA Instruments) with a base pressure of $\sim 10^{-8}$ Pa. Prior to sputtering the 99.999% purity Ni target was degassed by pre-sputtering. All the films were deposited at 100 °C with a UHV compatible magnetron source (Mighty Mak) in 99.9999% pure Ar. The epitaxial films were deposited at 0.2 Pa while the polycrystalline films were deposited at a pressure of 0.5 Pa. The deposition rate for both substrates was ~ 1.1 nm s^{-1}. Following deposition the films were annealed at 600 °C for 15 min in the vacuum chamber such that contamination was avoided and a stable microstructure was produced. The films were then cooled as rapidly as the apparatus would allow by switching off the substrate heater.

Microstructural characterisation

The microstructure of the films was assessed via a variety of techniques. A focussed ion beam (FIB, FEI 200 at 30 kV) microscope was used to investigate the grain size distribution of the polycrystalline films. FIB was also used to cut trenches down to the substrate such that the cross-section could also be imaged. X-ray diffraction was used to produce (111) pole figures of these films such that the in-plane texture could be determined. In addition to this, TEM (JEOL 2000FX at 200 kV and Phillips CM12 at 120 kV) plan-view samples were produced such that in situ testing and post-mortem analysis of the 200 nm polycrystalline film could be performed. The FIB micrographs and in some cases the TEM images were used to produce grain size statistics for each of the films. This was achieved by highlighting the grain boundaries on a transparency overlay and using imaging software (Leica, Quantimet Q500/W) to calculate the area of each grain, delivering a grain diameter for a circle of equivalent area. For each film thickness between 500 and 1200 grains were measured.

Electron backscatter diffraction (EBSD) was used in addition to FIB for the characterisation of the films on α-Al_2O_3. For this technique a field emission gun scanning electron microscope (FEG-SEM, LEO 1525) was used with an EBSD camera (EDAX) attached such that the local crystallographic alignment is determined. The data obtained by this method allows for the grain size and crystallographic texture of the films to be assessed.

Thermomechanical testing

The films were thermomechanically strained by two techniques. A self-made wafer curvature system using a laser to

[1] All films were deposited at the ZWE Thin Films, Max Planck Institute for Metals Research (Stuttgart), headed by Dr Thomas Wagner (deceased) at that time.

assess the substrate curvature was used to test complete wafers while monitoring the average stress. In addition, a heating stage for thermally straining some of the films in situ in the TEM was utilised to monitor dislocation activity during straining.

The wafer curvature system was used to cycle the films to 500 °C and back while recording the curvature of the substrate every 10 °C. The system was heated and cooled at 6 K min^{-1} with the exception of cooling below 100 °C where the rate was reduced to 4 K min^{-1} due to system limitations. The curvatures recorded during cycling, R_{meas}, were used alongside the substrate curvature measured prior to film deposition, R_{ref}, such that the film stress could be calculated via the Stoney relation [16]:

$$\sigma_f = \frac{M_s h_s^2}{6h_f}\left(\frac{1}{R_{meas}} - \frac{1}{R_{ref}}\right) \quad (1)$$

where M_s is the biaxial elastic modulus of the substrate, h_s is the substrate thickness and h_f the film thickness.

In order to perform thermomechanical tests in situ it was necessary to produce TEM specimens that could be thermally strained. 3-mm discs of the Si wafer were mechanically thinned from the reverse side. A HNO_3:HF:acetic acid mix in the ratio 2:1:1, which etches the Si and SiO_x but not the SiN_x, was then applied. This leaves a region of electron transparent Ni/SiN_x in the centre of the 3 mm disc. No hole is produced in the sample. As the Ni/SiN_x membrane is surrounded by a disc of Si wafer the strain due to thermal mismatch on heating of this sample corresponds to that for a full wafer. Should this membrane buckle under compressive stress numerous bend contours would be present in the TEM footage, such contours were not observed in the TEM results presented in this study. Further details of this type of in situ TEM experiment can be found in the literature [3, 17].

The stress state in the Ni in these TEM samples is expected to be somewhat different from those films completely adhered to Si due to a reduction in lateral constraint. However, due to the preservation of the SiN_x layer no change in the Ni free surfaces is produced. Both aspects validate a comparison of the in situ TEM experiments with the stress–temperature measurements recorded by the wafer curvature technique.

The thermal straining experiments in the TEM were performed by heating to a specified temperature. The heating rate of this set-up is rather quick with values of 10–50 K min^{-1}. The heating and cooling was done in a stepwise manner with holding times of several minutes at selected target temperatures. This resulted in a typical cycle time of less than 30 min, significantly faster than the ~120 min typical for a wafer curvature experiment. During thermal straining a high-speed CCD camera recorded video footage (at 25 frames/s) of the electron transparent region. Still images can then be extracted from the video for a frame by frame inspection.

Results

The polycrystalline films formed columnar microstructures, Fig. 1, with a very strong {111} fibre texture and log-normal grain size distributions. Table 1 gives a summary of the grain size distribution for the polycrystalline films on Si. The probability density function for the log-normal distribution is given below:

$$f = \frac{1}{x\sigma\sqrt{2\pi}}\exp\left(-\frac{(\ln x - \mu)^2}{2\sigma^2}\right) \quad (2)$$

here x is the random variable, grain diameter in this case, while μ and σ are, respectively, the mean and standard deviation of the corresponding Gaussian distribution. Presented in Fig. 2 is a cumulative distribution plot for the 400 nm film demonstrating the size distribution and fitting curve.

Grain size distribution analysis was also carried out on the 150 and 400 nm films after four thermal cycles to 500 °C. No changes in grain size were observed within the errors of the measurements.

The films deposited onto (0001) α-Al_2O_3 formed columnar microstructures in two broad, twin-related, alignments with the {111}-planes lying parallel to the interface. Due to the unusual grain growth caused by this partial epitaxy it proved difficult to determine a meaningful average grain size for these films. However, in all cases the smallest measured grain diameters were at least double the film thickness. In that case the film thickness rather than the grain size distribution will affect the mechanical properties.

In the thermomechanical testing the observed room temperature and high temperature (500 °C) flow stresses and the "thermoelastic" slopes, as illustrated in Fig. 3, were principally analysed.

Beginning with an examination of the results from the room temperature and 500 °C stresses. If the room temperature stress data for the films is plotted against inverse film thickness, following the Nix–Freund model, two regimes are observed: a linear increase in stress with inverse film thickness is observed initially and this is followed by a region in which the room temperature stress reaches a plateau, Fig. 4.

At 500 °C the stress data for the polycrystalline films also exhibits a double trend: a peak compressive stress is observed for the 600 nm film while the 150 and 1000 nm films exhibit significantly lower values of compressive stress, 150 and 250 MPa, respectively (Fig. 5). The 500 °C

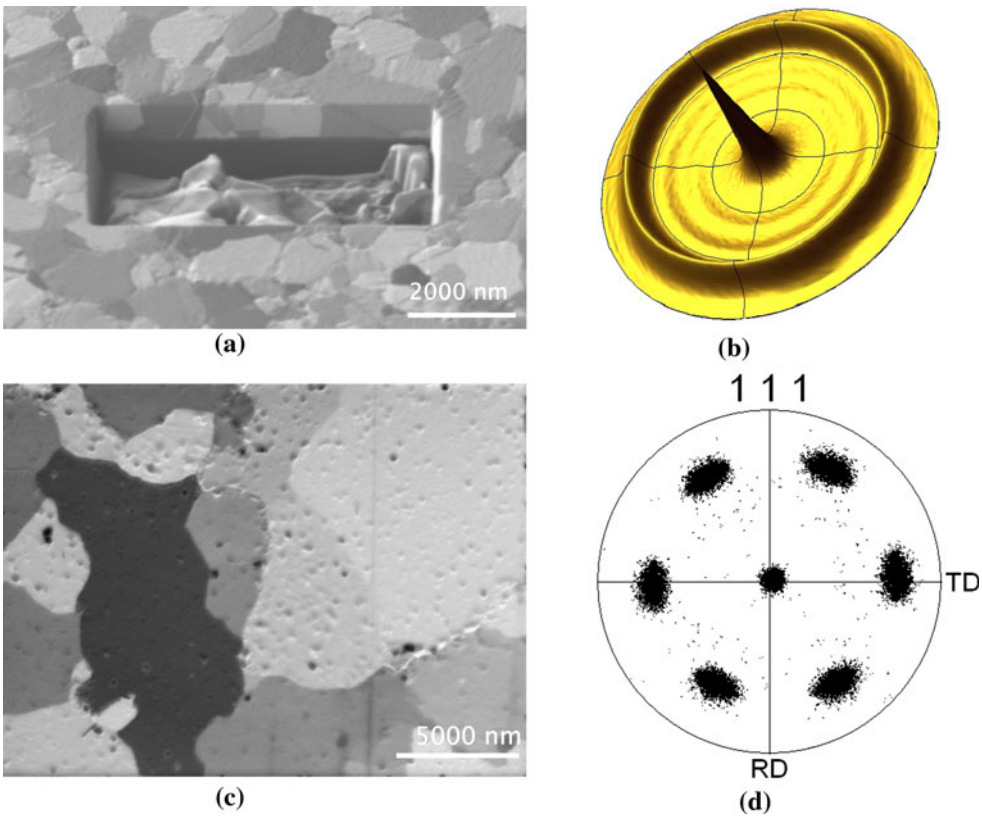

Fig. 1 Microstructures of the 1000-nm-thick polycrystalline (**a**, **b**) and epitaxial (**c**, **d**) films. **a** A FIB image of the polycrystalline film with a trench cut, the image was taken at 45° tilt. **b** An X-ray pole figure of the polycrystalline film showing the strong {111} fibre texture. **c** FIB micrograph of the epitaxial film, note the different scale bar. **d** EBSD pole figure illustrating the two broad grain alignments, each alignment produces four spots with the central spot shared

Table 1 Summary of log-normal distribution fit parameters for the polycrystalline films on Si. μ and σ are the mean and standard deviation of the corresponding Gaussian distribution

Film thickness (nm)	μ (nm)	σ
1000	1000 ± 30	0.50 ± 0.3
600	560 ± 6	0.51 ± 0.01
400	550 ± 20	0.54 ± 0.04
200	240 ± 7	0.52 ± 0.03
150	340 ± 10	0.60 ± 0.03

Fitting was carried out using Origin 8.0 software. In all cases at least 500 grains were analysed

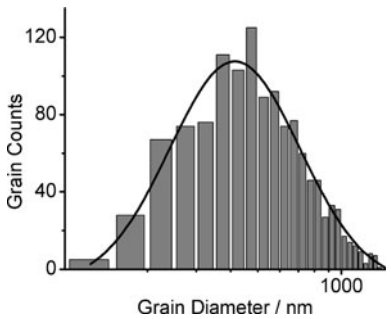

Fig. 2 Histogram of grain diameters for the 400-nm polycrystalline film. The *smooth line* is a software fit for a log-normal distribution

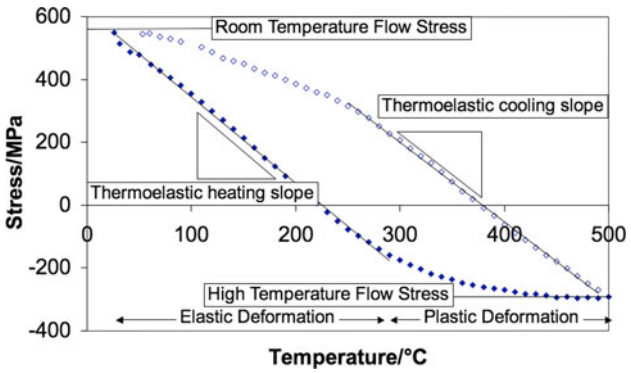

Fig. 3 Stress–temperature cycle for a 1000 nm Ni film on a SiN_x/SiO_x substrate illustrating the principal points of analysis. *Closed points* indicate the data recorded on heating of the films while *open points* indicate that collected on cooling

stress data for the films on α-Al_2O_3 are strongly linear with inverse film thickness.

In analysing the thermomechanical slopes we observe that thinner films exhibit values closer to those predicted from the mismatch in thermal expansivity. Figure 6 plots the mean value of the thermomechanical slopes observed for the films, as a percentage of that predicted from thermal expansivity mismatch, against the film thickness. For the range of film thicknesses studied here, the dependence appears linear and almost identical for the different

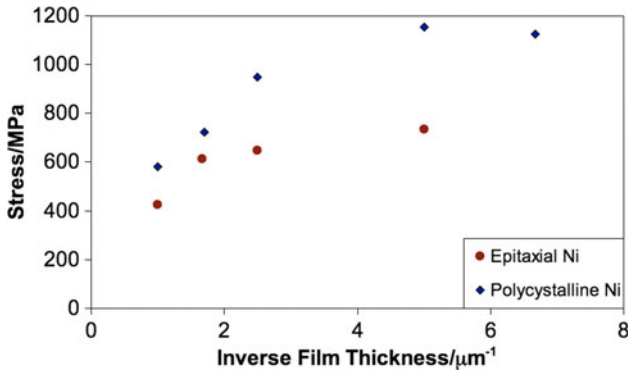

Fig. 4 A plot of the stress recorded in the films at room temperature at the end of the thermal cycles against the inverse film thickness. Note both Ni microstructures show an increase in stress with decreasing film thickness

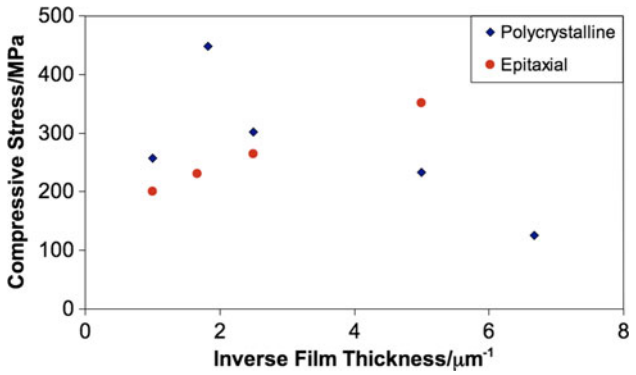

Fig. 5 The compressive stresses recorded in the films at 500 °C. The polycrystalline films clearly show a maximum at 600 nm while the compressive stress in the epitaxial films increases linearly with respect to inverse film thickness

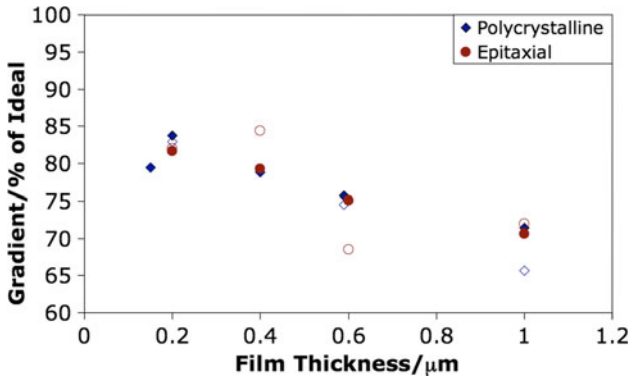

Fig. 6 Measured thermomechanical slopes on heating (*filled points*) the films from room temperature and cooling (*open points*) from 500 °C against the film thickness. Percentage values calculated from the following values: $\alpha_{Ni} = 13.4 \times 10^{-6}$ K^{-1}, $\alpha_{Si} = 3 \times 10^{-6}$ K^{-1}, $\alpha_{Al_2O_3} = 6 \times 10^{-6}$ K^{-1} and $M(\mathrm{Ni})_{(111)} = 390$ GPa

substrates. Somewhat lower values for both slopes were measured for the 150-nm-thick polycrystalline film compared to those seen for the 200 nm film. It is also not clear

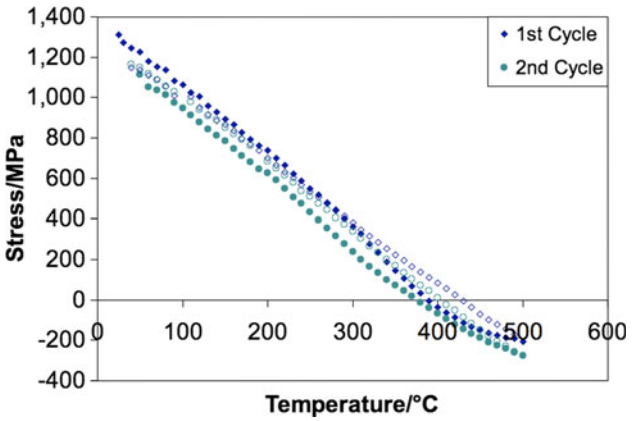

Fig. 7 The first two stress–temperature cycles recorded for the 200 nm film, the hysteresis observed here indicates a plastic strain of ~0.05%. *Closed symbols* correspond to the heating of the film to 500 °C while *open points* relate to cooling down to room temperature

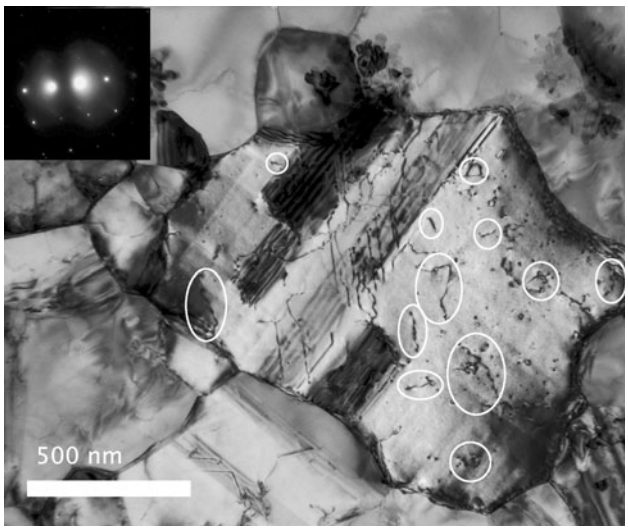

Fig. 8 TEM image of a grain in the 200 nm thick film prior to in situ testing, recorded with g_{200} conditions. All dislocations which were observed to glide during the in situ TEM experiment are *encircled*

why such a large difference is observed in the heating and cooling slopes of the 400 and 600 nm epitaxial films.

In performing the in situ testing of the 200 nm film it was common to see dislocation glide in the larger grains. This is despite the stress–temperature data for the 200 nm film showing very little deviation from the thermoelastic slopes, Fig. 7.

Figures 8 and 9 show two examples of large grains containing multiple dislocations in the 200 nm polycrstalline film. In these micrographs those dislocations that were observed to glide during in situ tests are indicated. In the course of three in situ tests on this 200 nm film it was generally observed that deformation was concentrated in such large grains. The plastic strain in such grains can be approximated by considering the displacement of Burgers

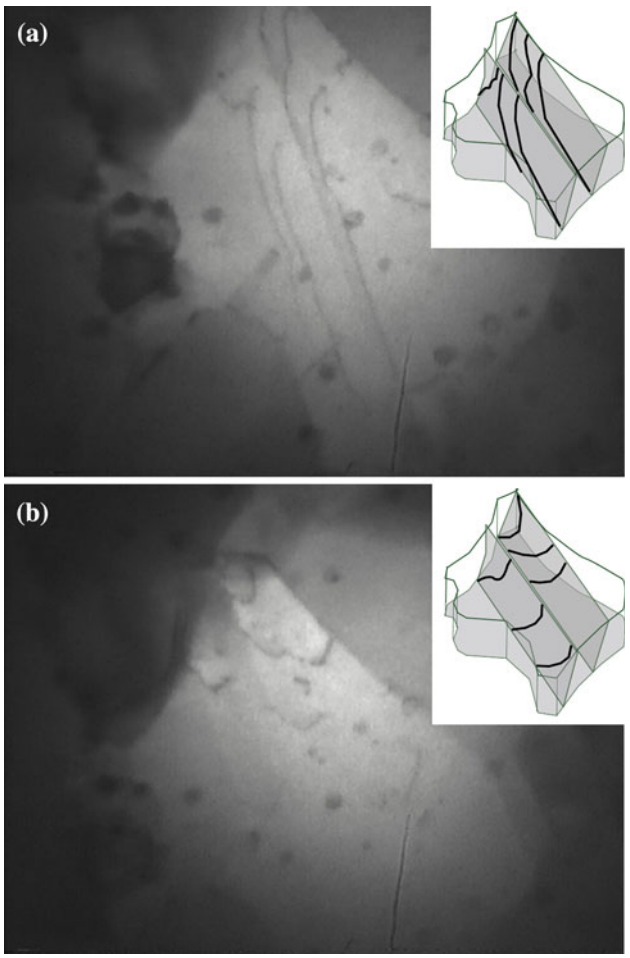

Fig. 9 Video captures from an in situ experiment on the 200 nm film. **a** shows the film during heating with six dislocations gliding along the length of the grain, **b** shows these dislocations gliding in the opposite direction during cooling. In both cases the *insert* provides a schematic depiction of the dislocations in the grain. The full video for this sequence can be found online at: http://www.oeaw.ac.at/esi/anims/200-nm-Ni-TEM-in-situ.mov

vectors associated with the glissile dislocations over the length of the grains. This analysis on three grains, 500–1200 nm diameter in size, observed during in situ heating showed that local strains in these grains were 0.10–0.20%, i.e. 2–4 times the global plastic strain for the film.

Discussion

The dependence of the room temperature flow stresses on film thickness is very similar to that found previously for other fcc films [3, 17]. By normalising the flow stresses with the shear modulus we can compare these results for Ni with those found previously for thermally strained polycrystalline Al and Cu, Fig. 10. This figure also plots a line for the flow stress predicted by the von Blanckenhagen [15] source model. This steep gain in flow stress followed by a

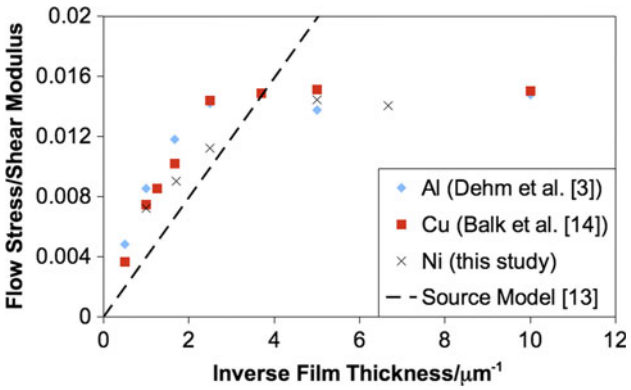

Fig. 10 A plot of room temperature yield data for Cu, Al and Ni on SiN_x/SiO_x substrates. For means of comparison the data has been normalised by their respective shear moduli (42 GPa for Cu, 25 GPa for Al and 80 GPa for Ni), versus the inverse film thickness. The *line* illustrates the prediction of the source model proposed by von Blanckenhagen et al.

plateau observed in the room temperature stresses can be explained by combining the work of von Blanckenhagen with that of Eiper et al. [18]. The flow stress rises steeply as the film thickness decreases and it becomes more difficult to activate dislocation sources but then the thermal strain exerted on the system (0.48% for Si substrates, 0.36% for α-Al_2O_3) becomes insufficient to cause general yielding of the films, leading to the plateau observed.

At high temperatures the double trend in the compressive flow stresses of the polycrystalline films can be explained by a competition between dislocation-mediated plasticity [15] and constrained diffusional creep [13, 14]. A similar phenomenon was observed by Wellner et al. [19] in thermomechanical testing of NiAl films. For films thicker than 600 nm plasticity is controlled predominantly by dislocation glide while the thinner polycrystalline films relax stresses through diffusive flow. This is most likely via constrained diffusional creep at grain boundaries proposed by Gao et al. [13, 14]. Further evidence for this can be seen in the stress–temperature cycles for the 150 and 200 nm films, Fig. 11. Both of these films exhibit an increase in the thermomechanical slope upon heating above 300 °C, although the effect is most pronounced for the 150 nm film. For this film the thermomechanical gradient changes from 3.3 to 7.3 MPa K^{-1}, almost double the upper theoretical limit of 3.9 MPa K^{-1} for Ni on Si. As such, it must be concluded that a process is operating to relieve stress in the film apart from the difference in thermal expansivity difference between the film and substrate. The observance of this process in only the thinner films and its applicability at high temperatures only points towards a diffusion effect involving surfaces and grain boundaries, i.e. thinner films have shorter diffusion paths and hence greater rates of deformation. This is further supported by the high temperature data for the epitaxial films. In these films a highly

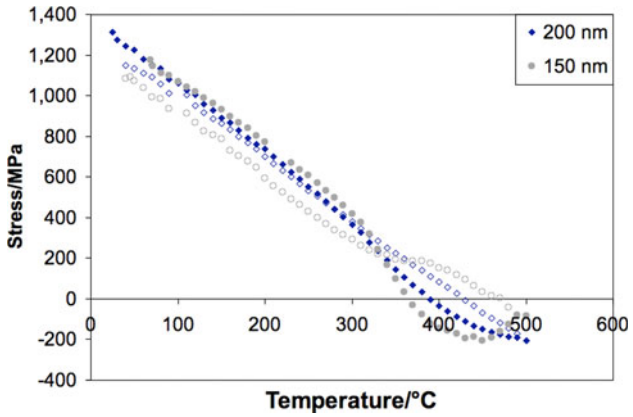

Fig. 11 Stress–temperature data for the first thermal cycles of the 150 and 200 nm films. Note the increase in gradient above 300 °C. *Closed points* indicate the data recorded on heating of the films while *open points* indicate that collected on cooling

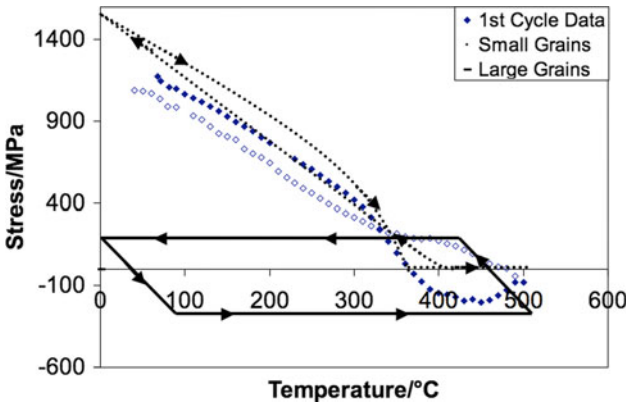

Fig. 12 The data for the first cycle of the 150 nm polycrystalline film alongside schematic representations of the stresses in larger grains and extremely small grains. It is assumed in this representation that the larger grains deform purely by dislocation glide while the small grains deform predominantly by diffusional processes. These represent the extremes of behaviour postulated here. In order to reconstruct the experimental data all intermediate grain sizes must be considered, this is not attempted. *Closed points* indicate the data recorded on heating of the films while *open points* indicate that collected on cooling

linear proportionality of the compressive flow stress to the inverse film thickness is observed. The grain sizes of the 200 and 400 nm epitaxial films are more than an order of magnitude larger than their polycrystalline counterparts, this greatly reduces the available diffusion paths and suppresses diffusion-controlled plasticity.

The ability of the 150 nm polycrystalline Ni film to maintain any compressive stress is, at first, confusing. If the tensile stress drops so rapidly above 300 °C, what is the driving force behind the continued drop of the stress into the compressive regime? A recent theory put forward by Rajagopalan et al. [20] may be able to explain this. The grain size distribution in the films ensures that the critical stress required to drive dislocation glide is not constant in all grains. If we apply the findings of von Blanckenhagen's [15] simulations we can say that the critical stress will be similar in grains whose diameter is larger than the film thickness but a grain whose diameter is less than the film thickness would be expected to have a higher critical stress. This is due to the finding that the smallest grain dimension dominates the mechanical properties. A film that has cooled from the deposition temperature would therefore be expected to contain a fraction of grains in which the stress has been relaxed somewhat by dislocation glide in addition to grains whose critical stress to initiate glide was not exceeded. In actual fact a full spectrum of behaviour is expected to have occurred with the larger grains having been subject to varying amounts of stress relaxation, however, it simplifies the problem to consider just a bimodal system of grains larger than the film thickness and grains significantly smaller. Yielding does not occur in tension within these small grains. The stress we observe via wafer curvature is then an average of these local stresses. By superimposing the effects of the dislocation-mediated plasticity in larger grains and the diffusion-mediated plasticity in smaller grains the schematic in Fig. 12 illustrates how the observed behaviour could arise. This tendency for smaller grains to support larger stresses has been directly observed by Phillips et al. [21] with micro-Laue X-ray diffraction.

The phenomenon of a film thickness dependent thermoelastic slope was also observed by Wellner [22] for NiAl films deforming plastically. Wellner also observed a change in the slope of the thermoelastic curve on cooling from different maximum strains. The thermoelastic slope on cooling is equivalent to a loading curve and hence a reduction in this slope from the thermoelastic limit indicates local plastic relief of stresses. The thermoelastic slope on heating is an unloading curve and hence any plastic flow driven by tensile stresses would be expected to *increase* this slope above the thermoelastic limit. However, while the thermoelastic slope on heating in Fig. 6 is steeper than that on cooling for the 600 and 1000 nm films the slopes are always lower than the thermoelastic limit. A possible explanation for this is if the relaxation in some large grains is so efficient that these grains enter a compressive stress regime while the average stress measured in the film is highly tensile. Yielding of these grains in compression would then lower the thermoelastic slope as observed.

This work therefore suggests that the mechanical properties of thin films are strongly dependent on the unusually large and unusually small grains, rather than the average grain. As a very strong {111} fibre texture is observed for these films and the films are subjected to a biaxial stress, leading to similar Schmid factors for all grains, it is expected that grain size is the determining factor in which grains exhibit plastic deformation. Further support for local

plastic deformation was found during the in situ tests. Figures 8 and 9 show two grains, both from the 200 nm polycrystalline film, in which extensive dislocation activity was observed in situ. These grains were, at between 500 and 1000 nm grain diameter, significantly larger than the average grain size of the films. The high degree of dislocation glide in these large grains on the edge of the distribution suggests that dislocation activity may be almost exclusively limited to such large grains.

Conclusion

The data presented here for the room and high temperature flow stresses fits in well with other results for similar materials, further supporting the conclusion that fcc metals behave in a very similar manner once material constants are accounted for.

The size effect observed in the thermomechanical gradients and the multiple dislocation glide seen in situ in the TEM support the conclusion that localised deformation in the form of dislocation glide is occurring in these films even in the apparently elastic regime. The size effect in this localised plasticity suggests that some critical grain size is required for such deformation. As such, thinner films contain fewer grains above this threshold and hence the thermoelastic slope approaches the theoretical value predicted by the thermal expansivity mismatch between the film and substrate.

Furthermore, the results of this study suggest that characterising thin films by their average grain size and attempting to rationalise the observed properties in relation to this average grain size may be too simplistic. If dislocation glide is only possible in grains above a critical size and diffusive flow possible only in the smaller grains then the grain size distribution of a film becomes a critical factor in that film's thermomechanical properties.

Acknowledgement Wafer curvature and in situ TEM were carried out at the Max Planck Institute for Metals Research, Stuttgart, during the authors' time there.

References

1. Nix WD (1989) Metall Trans A 20A:2217
2. Kobrinsky MJ, Thompson CV (2000) Acta Mater 48:625
3. Dehm G, Balk TJ, Edongué H, Arzt E (2003) Microelectr Eng 70:412
4. Vinci RP, Forrest SA, Bravman JC (2002) J Mater Res 17:1863
5. Baker SP, Keller-Flaig R-M, Shu JB (2003) Acta Mater 51:3019
6. Hall EO (1951) Proc R Soc London B 64:747
7. Petch NJ (1953) Iron Steel Inst 174:25
8. Black JR (1969) Proc IEEE 9:1587
9. Ohring M (2002) Materials science of thin films, 2nd edn. Academic Press, New York, p 735
10. Thompson CV, Carel R (1996) J Mech Phys Solids 44:657
11. Westmacott KH, Hinderberger S, Dahmen U (2001) Philos Mag A 81:1547
12. Freund LB (1987) J Appl Mech 54:553
13. Gao H, Zhang L, Nix WD, Thompson CV, Arzt E (1999) Acta Mater 47:2865
14. Weiss D, Gao H, Arzt E (2001) Acta Mater 49:2395
15. von Blanckenhagen B, Gumbsch P, Arzt E (2003) Philos Mag Lett 83:1
16. Stoney GG (1909) Proc R Soc London A 82:172
17. Balk TJ, Dehm G, Arzt E (2003) Acta Mater 51:221
18. Eiper E, Keckes J, Martinschitz K, Zizak I, Cabié M, Dehm G (2007) Acta Mater 55:1941
19. Wellner P, Dehm G, Kraft O, Arzt E (2004) Z Metallkd 95:769
20. Rajagopalan J, Han JH, Saif MTA (2008) Scripta Mater 59:734
21. Phillips MA, Spolenak R, Tamura N, Brown WL, MacDowell AA, Celestre RS, Padmore HA, Batterman BW, Arzt E, Patel JR (2004) Microelectr Eng 75:117
22. Wellner P (2003) Thermo-mechanical behaviour of NiAl thin films, Dissertation, Universität Stuttgart, p 65